

# P-WAVE PAIRING IN SUPERCONDUCTING $\text{Sr}_2\text{RuO}_4$

G. LITAK

*Department of Mechanics, Technical University of Lublin  
Nadbystrzycka 36, Lublin PL-20-618, Poland*

J.F. ANNETT, B.L. GYÖRFFY

*H.H. Wills Physics Laboratory, University of Bristol  
Tyndall Ave, Bristol BS8 1TL, United Kingdom*

K.I. WYSOKIŃSKI

*Institute of Physics, M. Curie-Skłodowska University,  
Radziszewskiego 10a, Lublin PL-20-031, Poland*

## 1. Introduction

Although there is strong evidence that  $\text{Sr}_2\text{RuO}_4$  is a triplet superconductor [2, 3], the full symmetry of the equilibrium state below  $T_c$  remains open to debate [2-14]. There exist strong indications for broken time-reversal symmetry in the superconducting state [15, 10] and equally convincing measurements showing that the order parameter  $\mathbf{d}(\mathbf{k})$  has a line of nodes on the Fermi surface [16-19]. The reason why this state of affairs represents a puzzle is that for all odd parity spin triplet pairing states in tetragonal crystals, group theory does not require the simultaneous presence of both broken time-reversal symmetry and line nodes [20]. To explain this inconsistency different three dimensional models of pairing have been proposed [11-13]. In fact the experimental results on heat transport [19] seem to favour the horizontal, with respect to (ab) crystal plane, line nodes. Usually in a multi-band BCS like model, with different coupling constants for each band, one generically finds multiple phase transitions as the different sheets of the Fermi surface are gaped on lowering the temperature. Since experimentally there is only one jump in the specific heat, at  $T_c = 1.5$  K, in constructing a sensible model one must eliminate such multiple transitions. Zhitomirsky and Rice [12], in their simplified two band model, considered an interaction which couple the order parameters of the different symmetry. The presence of this inter-band interaction leads to a single superconducting transition. Microscopically such coupling of different bands comes from

effective three site interactions. They assumed that one band in  $\text{Sr}_2\text{RuO}_4$  is the most important for superconducting pairing, while two other are gaped via an inter-band proximity effect. On the other hand Annett *et al.* [13] have proposed slightly different model. They considered a three orbital three dimensional model with effective in plane and out of plane nearest neighbour interactions, but did not allow for interactions mixing the symmetry of the order parameters. The price to pay in this model is the fine-tuning of two interactions in order to have a single superconducting transition at  $T_c \approx 1.5$  K. The calculations show that the model [13] explains quantitatively the  $T$  dependence of the specific heat, penetration depth and thermal conductivity without additional fitting parameters.

It is the purpose of this work to extend the model of Annett *et al.* [13] by allowing for symmetry mixing interactions. To this end we add small three point interaction to describe possible inter-orbital proximity effects.

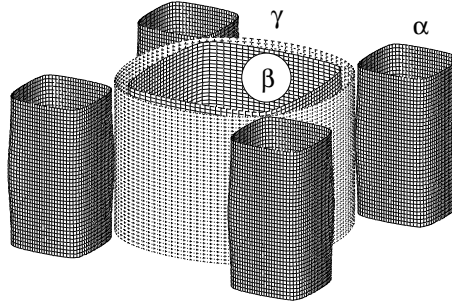


Figure 1. Calculated tight binding Fermi surface of  $\text{Sr}_2\text{RuO}_4$ .

## 2. The orbital model of superconductivity

To describe the superconducting state we use a simple multi-band attractive Hubbard model. Its Hamiltonian consists of two parts:

$$\hat{H} = \hat{H}_0 + \hat{H}_{int}, \quad (1)$$

where  $\hat{H}_0$  denotes the tight binding electron part corresponding to the experimentally observed band structure of  $\text{Sr}_2\text{RuO}_4$ .

$$\hat{H}_0 = \sum_{ijmm',\sigma} ((\varepsilon_m - \mu)\delta_{ij}\delta_{mm'} - t_{mm'}(ij)) \hat{c}_{im\sigma}^\dagger \hat{c}_{jm'\sigma}, \quad (2)$$

here  $m, m' = a, b, c$  refer to the three ruthenium  $t_{2g}$  orbitals  $a = xz$ ,  $b = yz$  and  $c = xy$  and  $i$  and  $j$  label the sites of a body centered tetragonal lattice.

$c_{im\sigma}^\dagger$  and  $c_{im\sigma}$  are the Fermion creation and annihilation operators for an electron on site  $i$  and orbital  $m$  with spin  $\sigma$ .

The hopping integrals  $t_{mm'}(ij)$  and site energies  $\varepsilon_m$  were fitted to reproduce the experimentally determined Fermi surface [21]. The calculated Fermi surface is shown in Fig. 1.

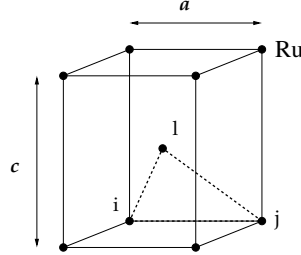


Figure 2. Body centered tetragonal lattice of Ru atoms in  $\text{Sr}_2\text{RuO}_4$ . Sites  $i$ ,  $j$ ,  $l$  correspond of possible realization of three nearest lattice sites. Note that two of sites must lie in  $\text{RuO}_2$  plane, while the third lies outside it.

The second part  $\hat{H}_{int}$  (Eq. 1) describes the general electron–electron interaction and can be written as

$$H_{int} = -\frac{1}{2} \sum_{ijlsmm'oo'\sigma\sigma'} U_{mm'oo'}^{\sigma\sigma'}(ijls) c_{im\sigma}^\dagger c_{jm'\sigma} c_{lo\sigma'}^\dagger c_{so'\sigma'}. \quad (3)$$

Some of the interaction constants  $U_{mm'oo'}^{\sigma\sigma'}(ijls)$  are assumed to be attractive: those acting between electrons on nearest neighbour sites with parallel spins and responsible for superconductivity. In Eq. 3 all site indices  $ijls$  can correspond, in general, to different sites but we assume, as is usually the case in an isotropic substance, that  $n$ -point interactions satisfy the relation

$$|U^{(n=1)}| > |U^{(n=2)}| > |U^{(n=3)}| > |U^{(n=4)}|. \quad (4)$$

A single point interaction ( $U^{(1)}$ ) refers, as usual, to the on-site repulsive Coulomb repulsion which does not contribute to electron pairing while the  $U^{(2)}$ , assumed to be attractive, represent the main contribution. The three point interaction coupling ( $U^{(3)}$ ) is apparently smaller than the bond term ( $U^{(2)}$ ), however its influence on pairing mechanism may be important [12], so we retain it, neglecting a four point coupling  $U^{(4)}$ .

Thus, the interaction part of Hamiltonian in our case reads:

$$\begin{aligned} \hat{H}_{int} = & -\frac{1}{2} \sum_{ijmm'\sigma\sigma'} U_{mm'}^{\sigma\sigma'}(ij) \hat{n}_{im\sigma} \hat{n}_{jm'\sigma'} \\ & -\frac{1}{2} \sum_{ijlmm'\sigma\sigma'} U_{mm',nn'}^{\sigma\sigma'}(ijl) c_{im'\sigma}^\dagger c_{jm\sigma} c_{ln'\sigma'}^\dagger c_{ln\sigma'}, \end{aligned} \quad (5)$$

where  $U_{mm'}^{\sigma\sigma'}(ij)$  (for  $i \neq j$ ) describe an attraction between electrons on the nearest sites with spins  $\sigma$  and  $\sigma'$  and in orbitals  $m$  and  $m'$  while  $U_{mm',oo'}^{\sigma\sigma'}(ijl)$  ( $i \neq j \neq l$ ) constant is the interaction (of any sign) between three nearest neighbour sites respectively (Fig. 2). It is called the assisted hopping term [22]. In our model, as will be discussed later, we assume that this term couples the in- and out-of- plane order parameters.

The actual calculations consist of solving, self-consistently, the following Bogoliubov-de Gennes equation:

$$\sum_{jm'\sigma'} \begin{pmatrix} E^\nu - H_{mm'}(ij) & \Delta_{mm'}^{\sigma\sigma'}(ij) \\ \Delta_{mm'}^{\sigma\sigma'*}(ij) & E^\nu + H_{mm'}(ij) \end{pmatrix} \begin{pmatrix} u_{jm'\sigma'}^\nu \\ v_{jm'\sigma'}^\nu \end{pmatrix} = 0, \quad (6)$$

where  $H_{mm'}(ij)$  is the normal spin independent part of the Hamiltonian, and the  $\Delta_{mm'}^{\sigma\sigma'}(ij)$  is self consistently given in terms of the pairing amplitude, or order parameter,  $\Delta_{mm'}^{\sigma\sigma'}(ij)$  is defined by the usual relation:

$$\begin{aligned} \Delta_{mm'}^{\sigma\sigma'}(ij) &= U_{mm'}^{\sigma\sigma'}(ij) \chi_{mm'}^{\sigma\sigma'}(ij) \\ &+ \sum_{loo'} U_{mm',oo'}(ijl) \chi_{oo'}^{\sigma\sigma'}(il), \end{aligned} \quad (7)$$

where

$$\chi_{mm'}^{\sigma\sigma'}(ij) = \sum_{\nu} u_{im\sigma}^\nu v_{jm'\sigma'}^{\nu*} (1 - 2f(E^\nu)), \quad (8)$$

and

$$f(E^\nu) = \frac{1}{1 + e^{\beta E^\nu}} \quad (9)$$

is Fermi function,  $\beta = 1/k_B T$ ,  $k_B$  is Boltzmann constant and  $\nu$  enumerates the solutions of Eq. 6.

### 3. Symmetry of order parameters

We solved the above system of Bogoliubov de Gennes equations (6-8) including all three bands and the experimental three dimensional Fermi surface (Fig. 1). We assumed that the pairing interaction  $U_{mm'}^{\sigma\sigma'}(ij)$  for nearest neighbours in plane is only acting for the  $c$  ( $d_{xy}$ ) Ru orbitals and the nearest neighbour inter plane interaction acts only in  $a$  and  $b$  orbitals ( $d_{xz}$ ,  $d_{yz}$ ). The motivation for this is that the dominant hopping integrals in plane are between  $c$  orbitals, and the largest out of plane hopping integrals are for  $a$  and  $b$ . On the other hand the additional three point, assisted hopping, interaction provides coupling between different orbitals  $a, b$  and  $c$ .

Therefore we have only three coupling constants  $U_{\parallel}$  and  $U_{\perp}$  describing these physically different interactions in- and off-plane and  $U_I$  which

correspond to inter-orbital coupling. Our strategy is to adjust these phenomenological parameters in order to obtain one transition at the experimentally determined  $T_c$ . Of course, this can be done for many choices of interactions parameters. Compare the results of our previous orbital model [13] with these obtained here for generalized orbital model with three point interactions taken into account.

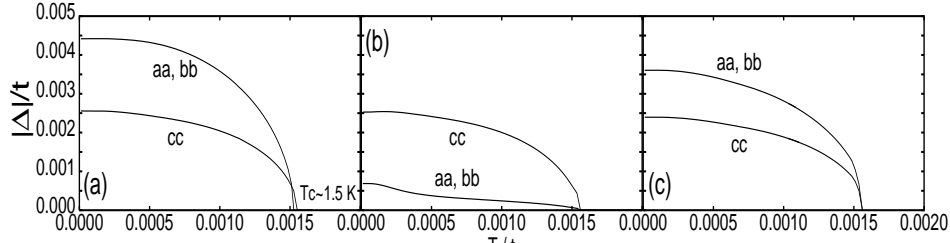


Figure 3. Order parameters,  $|\Delta_{aa}^x| = |\Delta_{bb}^x|$  and  $|\Delta_{cc}^x|$  as functions of temperature for various sets of interactions:  $U_\perp, U_\parallel, U_I$  ((a) for  $0.590t, 0.494t, 0.0$ ; (b) for  $0.400, 0.493t, 0.004t$ ; (c) for  $0.400t, 0.400t, 0.054t$ ; respectively; where  $t = 0.0816$  eV).

Because the pairing interactions  $U_{mm'}^{\sigma\sigma'}(ij)$  were assumed to act only for nearest neighbour sites in or out of plane, the pairing potential  $\Delta_{mm'}^{\sigma\sigma'}(ij)$  is also restricted to nearest neighbours. We further focus on only odd parity (spin triplet) pairing states for which the vector  $\mathbf{d} \sim (0, 0, d^z)$ , i.e.  $\Delta_{mm'}^{\uparrow\downarrow}(ij) = \Delta_{mm'}^{\downarrow\uparrow}(ij)$ , and  $\Delta_{mm'}^{\uparrow\uparrow}(ij) = \Delta_{mm'}^{\downarrow\downarrow}(ij) = 0$ . Therefore in general we have the following fourteen non-zero order parameters (i) for in plane bonds:  $\Delta_{cc}(\hat{\mathbf{e}}_x)$ ,  $\Delta_{cc}(\hat{\mathbf{e}}_y)$ , and (ii) for inter-plane bonds:  $\Delta_{aa}(\mathbf{R}_{ij})$ ,  $\Delta_{ab}(\mathbf{R}_{ij})$ ,  $\Delta_{bb}(\mathbf{R}_{ij})$  for  $\mathbf{R}_{ij} = (\pm a/2, \pm a/2, \pm c/2)$ .

Taking the lattice Fourier transform of Eq. 7 the corresponding p-wave pairing potentials in k-space have the general form of order parameter (suppressing the spin indices for clarity):

$$\Delta_{cc}(\mathbf{k}) = \Delta_{cc}^x \sin k_x + \Delta_{cc}^y \sin k_y \quad (10)$$

for the  $c$  orbitals and,

$$\Delta_{mm'}(\mathbf{k}) = \left( \Delta_{mm'}^x \sin \frac{k_x}{2} \cos \frac{k_y}{2} + \Delta_{mm'}^y \sin \frac{k_y}{2} \cos \frac{k_x}{2} \right) \cos \frac{k_z c}{2} \quad (11)$$

for  $m, m' = a, b$ . A more complete k-space analysis can be found in Appendix A.

Note that beyond the usual p-wave symmetry of the  $\sin k_x$  and  $\sin k_y$  type for the  $c$  orbitals, we include all three additional p-wave symmetries of the  $\sin k_i/2$  type which are induced by the effective attractive interactions between carriers on the neighboring out-of-plane Ru orbitals. These

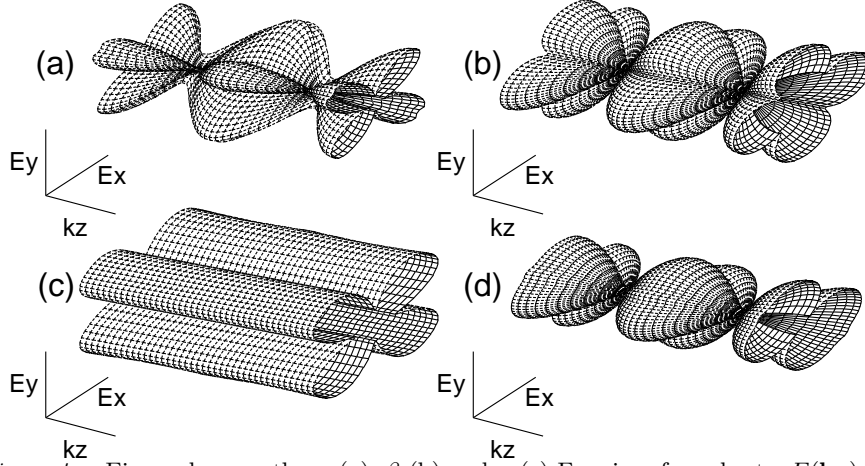


Figure 4. Eigenvalues on the  $\alpha$  (a),  $\beta$  (b) and  $\gamma$  (c) Fermi surface sheets,  $E(\mathbf{k}_F)$  along  $k_z$  direction for interactions chosen as in Fig. 3a, (d)  $E(\mathbf{k}_F)$  for  $\beta$  band Fermi surface and interactions chosen as in Fig. 3c ( $T = 0$ ).

interactions are also responsible for the f- and  $p_z$ -wave symmetry order parameters [13]. These relatively small components with smaller  $T_c$  will be neglected in this paper. The motivation comes from the strong impurity effects in the material [23].

We have solved Eqs. 6-8 for various sets of interactions:  $U_\perp$ ,  $U_\parallel$ ,  $U_I$ . For  $U_I = 0$  the order parameters have the symmetries  $\Delta_{cc}^y = i\Delta_{cc}^x$ ,  $\Delta_{bb}^y = i\Delta_{aa}^x$  as expected for a pairing symmetry [4] of  $(k_x + ik_y)\hat{e}_z$  type corresponding to the same time reversal broken pairing state as  $^3\text{He-A}$ . The off-diagonal components, such as  $\Delta_{ab}^x$  are small but non-zero, as are  $\Delta_{bb}^x$  and  $\Delta_{aa}^y$ . Note that the k-space pairing potentials  $\Delta_{mm'}(\mathbf{k})$  do not directly correspond to the energy gaps on the Fermi surface sheets, because the tight-binding Hamiltonian is non-diagonal in the orbital indices. Instead in Fig 4a-c we show the energy eigenvalues  $E_{\mathbf{k}}$  of our Hamiltonian evaluated at the Fermi surface for  $\alpha$ ,  $\beta$  and  $\gamma$  bands. One can see that there are horizontal circles around the cylindrical  $\beta$  Fermi surface sheet (Fig. 4b), while the order parameter at the  $\gamma$  sheet (Fig. 4c) is node-less. Interestingly, in our model  $\alpha$  sheet does not possess line nodes. Due to the small diagonal distortion of  $\alpha$  Fermi surface (Fig. 1) it has point nodes (Fig. 4a).

$U_\perp$ ,  $U_\parallel$ ,  $U_I$  were chosen in such way as to give a single transition with  $T_c = 1.5$  K. Figure 3a shows various  $\Delta$  obtained for our [13] orbital model ( $U_\perp = 0.590t$ ,  $U_\parallel = 0.494t$  but  $U_I = 0.0$ ). Here the interactions were tuned separately to give approximately the same  $T_c$ . All components of the order parameter in a,b and c orbitals are active.

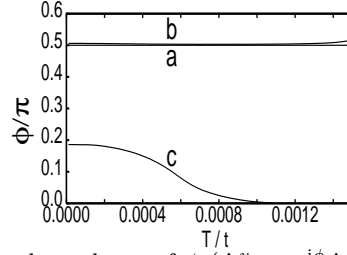


Figure 5. Temperature dependence of  $\phi$  ( $\Delta_{cc}^y = e^{i\phi} \Delta_{cc}^x$ ). Interaction parameters  $U_{\perp}$ ,  $U_{\parallel}$ ,  $U_I$  as in Fig. 3 for (a), (b) and (c); respectively. Note that for  $U_I = 0$  (a)  $\phi = \pi/2$  and  $\Delta_{cc}^y = i\Delta_{cc}^x$ .

In the case of Fig. 3b  $U_{\perp}$ ,  $U_{\parallel}$ ,  $U_I$  are equal to  $0.400t$ ,  $0.493t$ ,  $0.004t$ , respectively. Here a,b orbital order parameters  $\Delta_{aa}^x$ ,  $\Delta_{bb}^x$  have much smaller values than  $\Delta_{cc}^x$  and only due to small three point inter orbital coupling  $U_I$ . We have the proximity effect and hence a unique  $T_c$ .

In the last case  $U_{\perp}=0.400t$ ,  $U_{\parallel} = 0.400t$ ,  $U_I = 0.054t$  (Fig. 3c) the situation is different. To get  $T_c = 1.5K$  both interactions  $U_{\perp}$ ,  $U_{\parallel}$  take on smaller values comparing to those in Fig. 3a. The increase of the inter-orbital interaction  $U_I$  changes  $T_c$  and the values of  $\Delta_{mm}^i(T = 0)$  as well as their temperature dependence. The order parameters  $\Delta_{mm}^i$  fulfill more general relations  $\Delta_{cc}^x = e^{i\phi} \Delta_{cc}^y$  and  $\Delta_{bb}^x = e^{i\phi} \Delta_{aa}^y$ , where  $\phi$  is a temperature dependent phase. This dependence for all three cases are plotted in Fig. 5. For  $U_I = 0$   $\phi$  is constant and equal to  $\pi/2$  (curve a). A similar behaviour with  $\phi \approx \pi/2$  can be found for small  $U_I$  (curve b) while for relatively large  $U_I$  ( $U_I = 0.054t$ )  $\phi$  depends strongly on temperature (curve c). It is worthwhile to note that for low temperature  $T$  all order parameters are complex. It is also true for higher  $T$  but for  $U_I$  equal to 0 or relatively small. For larger interaction  $U_I$  there is a temperature  $T^*$  ( $T^* < T_c$ ) above which the order parameters are real. This is a source of additional vertical line nodes appearing at the Fermi surface. For  $U_I = 0.054t$  the horizontal line nodes are still present on the cylindrical  $\beta$  Fermi surface sheet (Fig. 4d). Due to  $\phi \neq \pi/2$  the eigenvalues on the Fermi surface show a two-fold symmetry instead of four-fold one present for  $U_I = 0$  (Fig. 4b).

To decide which of these three cases is closer to experiment we calculated the specific heat for the same interaction parameters as above using the relation:

$$C = -2k_B\beta^2 \sum_{m,\nu} E_{m,\nu} \frac{\partial f(E_{m,\nu})}{\partial \beta}. \quad (12)$$

In Figs. 6 a–c we have plotted the specific heat versus temperature. In all cases the low temperature limit of the specific heat is power law, because our gap parameters have line nodes on  $\beta$  Fermi surface sheet.

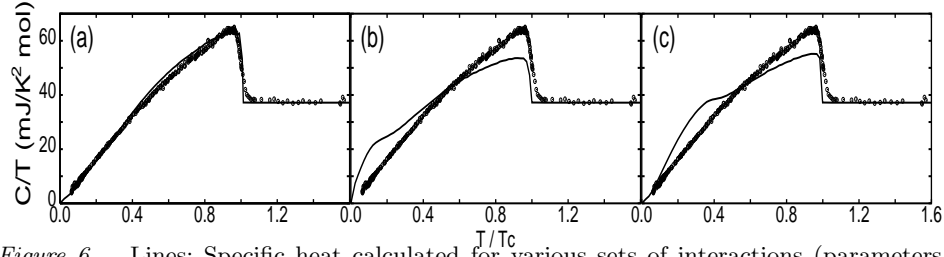


Figure 6. Lines: Specific heat calculated for various sets of interactions (parameters  $U_{\perp}$ ,  $U_{\parallel}$ ,  $U_I$  as in Fig. 3); full circles denote experimental data [16]

Going to larger temperatures we observe in Fig. 6a, that  $C$  has a discontinuity at  $T_c$  of 27mJ/mol, which is in agreement with the experiment [16, 13]. The slope of  $C/T$  versus  $T$  also comes out correctly. The values of the interaction parameters  $U_{\perp}$  and  $U_{\parallel}$  are in this model tuned to give single superconducting transition at temperature equal to 1.5 K. Interestingly, the two other figures (Fig. 6b-c) which correspond to the inter-orbital proximities have too small value of the specific heat jump at  $T_c$ . Technically it is due to different curvatures of temperatures dependences of  $\Delta_{mm'}$ .

#### 4. Summary and conclusions

In summary we would like to emphasize two points. Firstly, we have analyzed the orbital model of superconductivity with and without ‘inter-orbital proximity effect’. Both versions of the model allow for complex order parameter with line nodes on some of the Fermi surface sheets. Our description is a real space one with two point tight-binding interaction such as naturally arises in multi-band, extended, negative  $U$  Hubbard model [24].

Secondly, we wish to stress that in our original approach to the problem the parameters which describe the normal state are determined by fitting them to the very accurately known Fermi surface. The measured  $T_c$  determines both coupling constants  $U_{\parallel}$ ,  $U_{\perp}$ . As for the physical mechanism of pairing, the fact that  $U_{\perp} \approx U_{\parallel}$  implies that the pairing interaction is fairly isotropic in spite of the layered structure of the system. The model with “inter-orbital proximity” effect requires even more fine tuning of parameters in order to get correct slope and jump of the specific heat.

In conclusion, the scenario with active cc orbitals and “orbital proximity” mechanism for superconductivity in a and b orbitals is not consistent with specific heat data on  $\text{Sr}_2\text{RuO}_4$ .



## 5. Acknowledgements

This work was partially founded by the Committee of Scientific Research (Poland) through the grant KBN 2P03B 106 18, and the Royal Society (UK).

## 6. Appendix A

In case of a pure system one can take a Fourier transform of Eqs. (6-8). Thus

$$\sum_{m'\sigma'} \begin{pmatrix} E_{\mathbf{k}}^m - H_{mm'}(\mathbf{k}) & \Delta_{mm'}^{\sigma\sigma'}(\mathbf{k}) \\ \Delta_{mm'}^{\sigma\sigma'*}(\mathbf{k}) & E_{\mathbf{k}}^m + H_{mm'}(\mathbf{k}) \end{pmatrix} \begin{pmatrix} u_{\mathbf{k}m'\sigma'}^\nu \\ v_{\mathbf{k}m'\sigma'}^\nu \end{pmatrix} = 0, \quad (\text{A.1})$$

The gap equation (Eqs. 7-8) can be rewritten in k-space as

$$\begin{aligned} \Delta_{mm'}^{\sigma\sigma'}(\mathbf{k}) &= \frac{1}{N} \sum_{\mathbf{q}} U_{mm'}^{\sigma\sigma'}(\mathbf{k} - \mathbf{q}) \chi_{mm'}^{\sigma\sigma'}(\mathbf{q}) \\ &+ \frac{1}{N} \sum_{\mathbf{q}, oo'} U_{mm', oo'}(\mathbf{q}, \mathbf{k} - \mathbf{q}) \chi_{oo'}^{\sigma\sigma'}(\mathbf{q}). \end{aligned} \quad (\text{A.2})$$

and

$$\chi_{mm'}^{\sigma\sigma'}(\mathbf{k}) = u_{\mathbf{k}m\sigma} v_{\mathbf{k}m'\sigma'}^* (1 - 2f(E_{\mathbf{k}}^m)). \quad (\text{A.3})$$

In the orthogonal crystal (Fig. 2) various matrix elements of the interaction  $U$  responsible for p-wave paring can be written as

$$\begin{aligned} U_{cc}(\mathbf{k}, \mathbf{q}) &= 2U_{\parallel} V(\mathbf{k})V(\mathbf{q}) \\ U_{mm'}(\mathbf{k}, \mathbf{q}) &= 8U_{\perp} \tilde{V}(\mathbf{k})\tilde{V}(\mathbf{q}) && \text{for } m, m' = a, b \\ U_{mm'cc}(\mathbf{k}, \mathbf{k}') &= 8U_I \tilde{V}(\mathbf{k})V(\mathbf{q}) && \text{for } m', m = a, b \\ U_{ccmm'}(\mathbf{k}, \mathbf{q}) &= 8U_I V(\mathbf{k})\tilde{V}(\mathbf{q}) && \text{for } m', m = a, b \end{aligned} \quad (\text{A.4})$$

where  $V(\mathbf{k})$  and  $\tilde{V}(\mathbf{k})$  can be expressed as

$$\begin{aligned} V(\mathbf{k}) &= (\sin k_x + \sin k_y) \\ \tilde{V}(\mathbf{k}) &= \left( \sin \frac{k_x}{2} \cos \frac{k_y}{2} + \sin \frac{k_y}{2} \cos \frac{k_x}{2} \right) \cos \frac{k_z c}{2}. \end{aligned} \quad (\text{A.5})$$

Thus, the general form of order parameter

$$\Delta_{cc}(\mathbf{k}) = \Delta_{cc}^x \sin k_x + \Delta_{cc}^y \sin k_y \quad (\text{A.6})$$

for  $c$  orbitals and,

$$\Delta_{mm'}(\mathbf{k}) = \left( \Delta_{mm'}^x \sin \frac{k_x}{2} \cos \frac{k_y}{2} + \Delta_{mm'}^y \sin \frac{k_y}{2} \cos \frac{k_x}{2} \right) \cos \frac{k_z c}{2} \quad (\text{A.7})$$

for  $m, m' = a, b$  orbitals.

## 7. References

1. A. J. Leggett, Rev. Mod. Phys, **47** 331 (1975).
2. Y.Maeno, T.M. Rice and M. Sigrist, Physics Today **54**, 42 (2001).
3. A. Mackenzie and Y. Maeno, Physica **B280**, 148 (2000).
4. D. F. Agterberg, T. M. Rice and M. Sigrist, Phys. Rev. Lett. **73** 3374 (1997).
5. I. I. Mazin and D. J. Singh, Phys. Rev. Lett. **79** 733 (1997).
6. K. Miyake and D. Narikiyo, Phys. Rev. Lett. **83** (1999).
7. M.J. Graf and A.V. Balatsky, Phys. Rev. b **62**, 9697 (2000).
8. H. Won and K. Maki, Europhys. Lett. **52**, 427 (2000).
9. T. Dahm, H. Won, and K. Maki, cond-mat/0006301.
10. M. Sigrist, Physica **B280** 154 (2000).
11. Y. Hasegawa, K. Machida and M. Ozaki, J. Phys. Japan **69**, 336 (2000).
12. M. E. Zhitomirsky and T. M. Rice, Phys. Rev. Lett. **87**, 057001 (2001).
13. J.F. Annett, G. Litak, B.L. Györfy, K.I. Wysokiński, preprint cond-mat/0109023.
14. I. Eremin, D. Manske, C. Joas and K.H. Bennemann, preprint cond-mat/0102074.
15. G.M. Luke, Y. Fudamoto, K.M. Kojima *et al.* Nature **394** 558 (1998).
16. S. NishiZaki, Y. Maeno and Z. Mao, J. Phys. Japan **69**, 336 (2000).
17. I. Bonalde, B.D. Yanoff, M.B. Salamon *et al.*, Phys. Rev. Lett. **85**, 4775 (2000).
18. C. Lupien, W.A. MacFarlane, C. Proust *et al.*, Phys. Rev. Lett. **86**, 5986 (2001).
19. M.A. Tanatar, M. Suzuki, S. Nagai *et al.*, Phys. Rev. Lett. **86** 2649 (2001).
20. J.F. Annett, Adv. Phys. **39**, 83 (1990).
21. C. Bergemann, S. R. Julian, A.P. Mackenzie *et al.*, Phys. Rev. Lett. **84** 2662 (2000).
22. D.L. Cox and A. Zawadowski, *Exotic Kondo Effects in Metals*, (Taylor and Francis, London 1999).
23. A.P. Mackenzie, R.K.W. Haselwimmer, A.W. Tyler *et al.*, Phys. Rev. Lett. **80** (1998) 161.
24. R.Micnas, J.Ranninger and S.Robaszkiewicz, Rev. Mod. Phys. **62**, 113 (1991).